

DOI:10.13409/j.cnki.jdpme.20191017001

双圆形衬砌隧洞对柱面SH波作用下附近场地动力响应的影响分析*

周凤玺^{1,2}, 梁玉旺¹, 庞宾宾¹

(1. 兰州理工大学土木工程学院, 甘肃 兰州 730050; 2. 西部土木工程防灾减灾教育部工程研究中心, 甘肃 兰州 730050)

摘要: 在柱面SH波作用下, 由于弹性半空间中存在水平和垂直平行双圆形衬砌隧道, 附近场地的动力响应将会受到影响。因此, 本文基于弹性波理论, 采用波函数展开法分析了双隧洞周围的柱面SH波散射问题, 给出了双圆形衬砌隧道附近场地的位移解析解, 并验证了该解的收敛性。通过对衬砌隧道的衬砌刚度、隧洞埋深、两隧洞的中心间距以及入射波频率等参数的分析, 研究了双圆形衬砌隧洞附近场地土体的位移幅值沿水平方向和深度方向的变化规律。结果表明: 衬砌刚度、隧洞埋深、中心间距以及入射频率对双圆形衬砌隧洞附近场地的动力响应有着显著的影响。

关键词: 柱面SH波; 双圆形衬砌隧洞; 散射; 场地位移

中图分类号: P315.3 **文献标识码:** A **文章编号:** 1672-2132(2021)02-0276-11

Influence Analysis of Double Circular Lined Tunnel on Near-Field Dynamic Response of Cylindrical SH Waves

ZHOU Fengxi^{1,2}, LIANG Yuwang¹, PANG Binbin¹

(1. School of Civil Engineering, Lanzhou University of Technology, Lanzhou 730050, China;

2. Engineering Research Center of Disaster Mitigation in Civil Engineering of Ministry of Education, Lanzhou 730050, China)

Abstract: Under the action of cylindrical SH waves, the dynamic response of the nearby site will be affected by the horizontal and vertical parallel double circular lined tunnels in the elastic half space. Therefore, based on elastic wave theory, the problem of cylindrical SH wave diffraction around double circular lined cavity is analyzed using the wave function expansion method. The displacement analytical solution of the site near the double circular lined tunnel is presented, and the precision of the solution is verified. Through the analysis on the lining stiffness, the burial depth of the cavity, the center distance between the two cavities, the frequency of the incident wave, etc., the variation of the displacement amplitude of the soil near the double circular lined tunnel in the horizontal and vertical directions is studied. It is shown that the lining stiffness, burial depth, center distance and incident frequency have significant effects on the dynamic response of the site near the double circular lined tunnel.

Keywords: cylindrical SH wave; double circular lined tunnel; scattering; dynamic response

* 收稿日期: 2019-09-17; 修回日期: 2019-12-04

基金项目: 国家自然科学基金项目(51978320; 11962016)、甘肃省基础研究创新群体(20JR5RA478)资助

作者简介: 周凤玺(1979—), 男, 教授, 博士。主要从事岩土力学和复合材料结构力学方面的研究工作。

E-mail: geolut@163.com

引言

近年来,一些大城市为了解决土地资源紧缺、交通拥堵等问题而大力修建综合管廊、地铁隧道等地下结构。然而,地下结构的修建会对附近场地的地动力响应产生一定的影响,继而会给附近已有建筑物以及拟建工程结构的抗震设计带来影响。综合管廊、地铁隧道通常需要修建两个或两个以上的隧道。因此,研究地震波作用下地下双圆衬砌隧洞对附近场地的动力响应在地表以及地下沿深度的变化规律具有重要的意义。

通过波函数展开法, Y. H. Pao 等^[1]早在 1973 年就创造性地研究了在弹性波入射下全空间中非衬砌洞室的动应力集中问题,之后,很多学者相继针对于衬砌结构本身的地震动响应问题,对弹性波散射问题进行了大量研究,取得丰硕的研究成果^[2-8],而在地下隧洞修建后引起附近场地动力响应变化方面的问题研究较少。为此,关于半空间中地下衬砌结构对地表地震动问题,梁建文等^[9-12]分析了地下圆形隧道在多种弹性波入射下对地表运动幅值的影响。采用一种高精度的间接边界积分方程法,梁建文等^[13-14]研究了平面 P-SV 波作用下任意形状衬砌洞室的散射问题和动力响应问题。结果表明,地下隧洞的修建会对地表面的动力响应产生一定的放大效应。再次采用波函数展开法,梁建文等^[15-17]研究了半空间中双洞室在 P 波、SV 波等平面波入射下地面动力响应问题并且给出了相应的级数解答。其研究表明,由于洞室之间的相互影响,地下双洞室的动力响应较单洞室的动力响应有更显著的放大作用,同时对沿线地面运动也具有显著的放大作用。H. Alielahi 等^[18]以及 Zh. X. Liu 等^[19]通过边界单元法(BEM),分别研究了水平方向平行双隧洞和竖直重叠双隧洞在 P-SV 波入射下对附近表面动力响应的影响。结果表明,隧洞等地下结构对场地附近的动力响应有明显的放大作用,地下室群对附近表面地震动的影响也应该在工程设计的考虑范围之内。

综上所述,目前的研究成果大部分针对于平面波(即远场地震)作用下衬砌结构本身以及结构对地表地震动响应的分析,而对于柱面波(近场地震)作用下地下衬砌结构对周围土体在深度方向

的动力响应影响,尤其是考虑双衬砌隧洞的研究并不多见。因此,本文以地下双圆形衬砌隧洞为研究对象,并将半空间介质视为弹性介质分析了柱面 SH 波作用下场地位移的变化情况,在庞宾宾^[20]研究的基础上,通过对双圆形隧洞的衬砌刚度、埋深、中心间距和入射波圆频率等参数分析,对双隧洞附近场地的土体位移幅值沿水平方向和深度方向的变化规律分别进行研究。

1 数学模型

参照文献[20],建立了水平平行布置和竖向重叠布置的两个双圆衬砌隧洞的数学模型分别如图 1、图 2 所示。

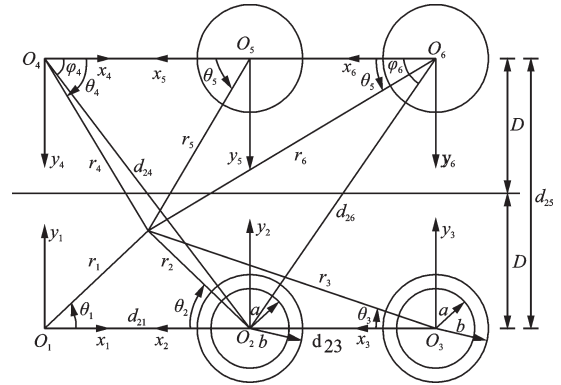


图 1 水平方向设置的双圆形衬砌隧洞

Fig.1 Double circular lined tunnels in horizontal direction

在两个模型中,双圆形衬砌隧洞的埋深为 D ,内半径和外半径分别为 a 和 b ,两隧洞的衬砌属性由 Lamé 常数 λ_1 、 μ_1 和密度 ρ_1 来表示;半空间为各向同性的均匀弹性介质,其属性由 Lamé 常数 λ 、 μ 和密度 ρ 来表示。设坐标 O_1 (直角坐标为 (x_1, y_1) ,极坐标为 (r_1, θ_1) ,其中 θ_1 是 r_1 与 x_1 的夹角。下文中坐标表示方法与该坐标表示方法相同)处有一柱面 SH 波的入射波波源, O_2 处和 O_3 处为双圆形衬砌隧洞中心, d_{12} 为波源与左隧洞中心的距离, d_{23} 为两隧洞的中心间距。由于镜像法原理^[18]的使用,半空间模型问题转换为全空间模型问题,地表处的直边界条件将自动满足,从而使求解过程得到简化,其中坐标系 O_1 、 O_2 和 O_3 镜像后的等效坐标体系为坐标系 O_4 、 O_5 和 O_6 。

从波源 O_1 处产生的柱面 SH 波,根据其传播特性可以表示为:

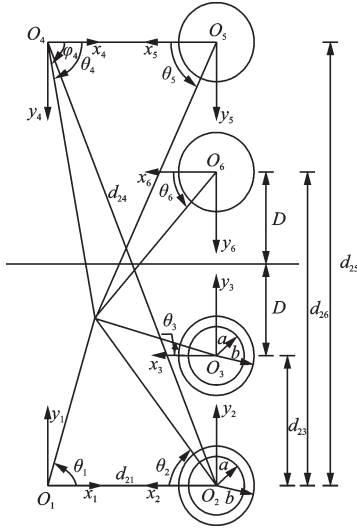


图2 竖直方向设置的双圆形衬砌隧洞

Fig.2 Double circular lined tunnels in vertical direction

$$W_{i1}^{(1)}(r_1, \theta_1) = \omega_0 H_0^{(1)}(kr_1) \exp(-i\omega t) \quad (1)$$

式中, ω_0 为入射柱面 SH 波的位移幅值; $H_0^{(1)}$ 为第一类 0 阶 Hankel 函数; ω 为入射波的圆频率, $k = \omega/\beta$ 为波数, 其中, $\beta = \sqrt{\mu/\rho}$ 为波速; $i = \sqrt{-1}$ 为虚数单位; t 为时间; 为了不失一般性, 取 $\omega_0 = 1$, 同时略去时间因子 $e^{-i\omega t}$, 则入射波的势函数可简化为:

$$W_{i1}^{(1)}(r_1, \theta_1) = H_0^{(1)}(kr_1) \quad (2)$$

地表边界处在入射波 $W_{i1}^{(1)}$ 作用下会产生反射波, 而隧洞衬砌外边界在入射波 $W_{i1}^{(1)}$ 作用下会产生散射波。入射波、反射波和散射波的合形成了半空间介质中的总波场 W , 并且满足如下波动方程:

$$\frac{\partial^2 W}{\partial r^2} + \frac{1}{r} \frac{\partial W}{\partial r} + \frac{1}{r^2} \frac{\partial^2 W}{\partial \theta^2} = \frac{1}{\beta^2} \frac{\partial^2 W}{\partial t^2} \quad (3)$$

同时, 入射 $W_{i1}^{(1)}$ 作用于衬砌外边界时, 在衬砌内部还会产生折射波, 进而还会散射波, 因此, 衬砌介质中总波场 W_L 由折射波和散射波共同构成, 并且满足如下波动方程:

$$\frac{\partial^2 W_L}{\partial r^2} + \frac{1}{r} \frac{\partial W_L}{\partial r} + \frac{1}{r^2} \frac{\partial^2 W_L}{\partial \theta^2} = \frac{1}{\beta_1^2} \frac{\partial^2 W_L}{\partial t^2} \quad (4)$$

其中, $\beta_1 = \sqrt{\mu_1/\rho_1}$, 是柱面 SH 波在衬砌介质内的波速。

2 介质中的波场

2.1 半空间介质中的波场

采用分离变量法求解波动方程(3), 可以得到

满足 Sommerfeld 辐射条件的散射位移场。可表示为:

$$W_{s2}^{(2)}(r_2, \theta_2) = \sum_{n_2=0}^{+\infty} H_{n_2}^{(1)}(kr_2) (A_{s2, n_2} \cos n_2 \theta_2 + B_{s2, n_2} \sin n_2 \theta_2) \quad (5)$$

$$W_{s3}^{(3)}(r_3, \theta_3) = \sum_{n_3=0}^{+\infty} H_{n_3}^{(1)}(kr_3) (A_{s3, n_3} \cos n_3 \theta_3 + B_{s3, n_3} \sin n_3 \theta_3) \quad (6)$$

其中, $A_{s2, n_2}, B_{s2, n_2}, A_{s3, n_3}$ 和 B_{s3, n_3} 为待定系数, $H_n^{(1)}(x)$ 为第一类 n 阶 Hankel 函数。

采用镜像法原理^[18], 地表以上等效的波势函数表达式可表示如下:

$$W_{r4}^{(4)}(r_4, \theta_4) = H_0^{(1)}(kr_4) \quad (7)$$

$$W_{s5}^{(5)}(r_5, \theta_5) = \sum_{n_5=0}^{+\infty} H_{n_5}^{(1)}(kr_5) (A_{s5, n_5} \cos n_5 \theta_5 + B_{s5, n_5} \sin n_5 \theta_5) \quad (8)$$

$$W_{s6}^{(6)}(r_6, \theta_6) = \sum_{n_6=0}^{+\infty} H_{n_6}^{(1)}(kr_6) (A_{s6, n_6} \cos n_6 \theta_6 + B_{s6, n_6} \sin n_6 \theta_6) \quad (9)$$

式中, A_{s2, n_2}, B_{s2, n_2} 的值与 A_{s5, n_5}, B_{s5, n_5} 的值对应相等, A_{s3, n_3}, B_{s3, n_3} 的值与 A_{s6, n_6}, B_{s6, n_6} 的值对应相等。

因此, 半空间介质中总波场表示为:

$$W = W_{i1}^{(1)}(r_1, \theta_1) + W_{s2}^{(2)}(r_2, \theta_2) + W_{s3}^{(3)}(r_3, \theta_3) + W_{r4}^{(4)}(r_4, \theta_4) + W_{s5}^{(5)}(r_5, \theta_5) + W_{s6}^{(6)}(r_6, \theta_6) \quad (10)$$

2.2 衬砌介质中的波场

对波动方程(4)分别在极坐标系 (r_2, θ_2) 和极坐标系 (r_3, θ_3) 下使用分离变量法进行求解, 可以分别得到隧洞 O_2 和隧洞 O_3 衬砌内散射波和折射波产生的位移场, 其分别表示为:

$$W_{L1}^{(2)}(r_2, \theta_2) = \sum_{n_2=0}^{+\infty} H_{n_2}^{(1)}(k_1 r_2) (C_{L1, n_2} \cos n_2 \theta_2 + D_{L1, n_2} \sin n_2 \theta_2) \quad (11)$$

$$W_{L2}^{(2)}(r_2, \theta_2) = \sum_{n_2=0}^{+\infty} J_{n_2}(k_1 r_2) (C_{L2, n_2} \cos n_2 \theta_2 + D_{L2, n_2} \sin n_2 \theta_2) \quad (12)$$

$$W_{L3}^{(3)}(r_3, \theta_3) = \sum_{n_3=0}^{+\infty} H_{n_3}^{(1)}(k_1 r_3) (C_{L3, n_3} \cos n_3 \theta_3 + D_{L3, n_3} \sin n_3 \theta_3) \quad (13)$$

$$W_{L4}^{(3)}(r_3, \theta_3) = \sum_{n_3=0}^{+\infty} J_{n_3}(k_1 r_3) (C_{L4, n_3} \cos n_3 \theta_3 + D_{L4, n_3} \sin n_3 \theta_3) \quad (14)$$

因此, 左隧洞、右隧洞以及下隧洞、上隧洞衬砌

介质内的波场分别表示为：

$$W_{LL} = W_{L1}^{(2)}(r_2, \theta_2) + W_{L2}^{(2)}(r_2, \theta_2) \quad (15)$$

$$W_{LR} = W_{L3}^{(3)}(r_3, \theta_3) + W_{L4}^{(3)}(r_3, \theta_3) \quad (16)$$

$$W_{LB} = W_{L1}^{(2)}(r_2, \theta_2) + W_{L2}^{(2)}(r_2, \theta_2) \quad (17)$$

$$W_{LA} = W_{L3}^{(3)}(r_3, \theta_3) + W_{L4}^{(3)}(r_3, \theta_3) \quad (18)$$

3 问题的求解

3.1 引入边界条件

如前所述地表处的零应力边界条件自动满足，因此，所求问题相应的边界条件为^[7]：

(1) 零应力边界条件(衬砌内表面处)：

$$\left. \frac{\partial W_{LL}}{\partial r_2} \right|_{r_2=a} = \left. \frac{\partial W_{LR}}{\partial r_3} \right|_{r_3=a} = 0, \quad \left. \frac{\partial W_{LB}}{\partial r_2} \right|_{r_2=a} = \left. \frac{\partial W_{LA}}{\partial r_3} \right|_{r_3=a} = 0 \quad (19)$$

(2) 应力连续条件(衬砌与半空间交界面处)：

$$\mu_1 \left. \frac{\partial W_{LL}}{\partial r_2} \right|_{r_2=b} = \mu \left. \frac{\partial W}{\partial r_2} \right|_{r_2=b}, \quad \mu_1 \left. \frac{\partial W_{LR}}{\partial r_3} \right|_{r_3=b} = \mu \left. \frac{\partial W}{\partial r_3} \right|_{r_3=b} \quad (20)$$

$$\mu_1 \left. \frac{\partial W_{LB}}{\partial r_2} \right|_{r_2=b} = \mu \left. \frac{\partial W}{\partial r_2} \right|_{r_2=b}, \quad \mu_1 \left. \frac{\partial W_{LA}}{\partial r_3} \right|_{r_3=b} = \mu \left. \frac{\partial W}{\partial r_3} \right|_{r_3=b} \quad (21)$$

(3) 位移连续条件(衬砌与半空间交界面处)：

$$W_{LL}|_{r_2=b} = W|_{r_2=b}, \quad W_{LR}|_{r_3=b} = W|_{r_3=b} \quad (22)$$

$$W_{LB}|_{r_2=b} = W|_{r_2=b}, \quad W_{LA}|_{r_3=b} = W|_{r_3=b} \quad (23)$$

3.2 问题的解答

为了求解待定系数，需要利用 Graf 公式将不同坐标系下的波函数转换在同一坐标 (r_2, θ_2) 中来，然后代入边界条件进行求解，具体如下：

$$E_6(n_2, b) \cdot (A_{i1, n2}^* + A_{s3, n2}^* + A_{r4, n2}^* + A_{s5, n2}^* + A_{s6, n2}^*) + E_5(n_2, b) \cdot A_{s2, n2} - \frac{\mu_1}{\mu} \cdot E_9(n_2, b) \cdot C_{L1, n2} = 0 \quad (24)$$

$$E_6(n_2, b) \cdot (B_{s3, n2}^* + B_{r4, n2}^* + B_{s5, n2}^* + B_{s6, n2}^*) + E_5(n_2, b) \cdot B_{s2, n2} - \frac{\mu_1}{\mu} \cdot E_9(n_2, b) \cdot D_{L1, n2} = 0 \quad (25)$$

$$E_6(n_2, b) \cdot (A_{i1, n2}^* + A_{s3, n2}^* + A_{r4, n2}^* + A_{s5, n2}^* + A_{s6, n2}^*) + E_5(n_2, b) \cdot A_{s2, n2} - \frac{\mu_1}{\mu} \cdot E_8(n_2, b) \cdot C_{L3, n2} = 0 \quad (26)$$

$$E_6(n_2, b) \cdot (B_{s3, n2}^* + B_{r4, n2}^* + B_{s5, n2}^* + B_{s6, n2}^*) + E_5(n_2, b) \cdot B_{s2, n2} - \frac{\mu_1}{\mu} \cdot E_8(n_2, b) \cdot D_{L3, n2} = 0 \quad (27)$$

$$(A_{i1, n2}^* + A_{s3, n2}^* + A_{r4, n2}^* + A_{s5, n2}^* + A_{s6, n2}^*) \cdot J_{n_2}(kb) + A_{s2, n2} \cdot H_{n_2}^{(1)}(kb) - C_{L1, n2} \cdot G_1(k_1 b) = 0 \quad (28)$$

$$(B_{s3, n2}^* + B_{r4, n2}^* + B_{s5, n2}^* + B_{s6, n2}^*) \cdot J_{n_2}(kb) + B_{s2, n2} \cdot H_{n_2}^{(1)}(kb) - D_{L1, n2} \cdot G_1(k_1 b) = 0 \quad (29)$$

$$(A_{i1, n2}^* + A_{s3, n2}^* + A_{r4, n2}^* + A_{s5, n2}^* + A_{s6, n2}^*) \cdot J_{n_2}(kb) + A_{s2, n2} \cdot H_{n_2}^{(1)}(kb) - C_{L3, n2}^* \cdot J_{n_2}(k_1 b) = 0 \quad (30)$$

$$(B_{s3, n2}^* + B_{r4, n2}^* + B_{s5, n2}^* + B_{s6, n2}^*) \cdot J_{n_2}(kb) + B_{s2, n2} \cdot H_{n_2}^{(1)}(kb) - D_{L3, n2}^* \cdot J_{n_2}(k_1 b) = 0 \quad (31)$$

方程组(24)~(31)推导过程详见附录，并且通过对方程组(24)~(31)化简整理(具体推导过程详见附录)，可以得到关于 $A_{s2, n2}$ 、 $B_{s2, n2}$ 、 $A_{s3, n2}$ 、 $B_{s3, n2}$ 四个待定系数的无穷阶线性代数方程组：

$$\sum_{j=0}^{+\infty} \begin{bmatrix} E11 & E12 & E13 & E14 \\ E21 & E22 & E23 & E24 \\ E31 & E32 & E33 & E34 \\ E41 & E42 & E43 & E44 \end{bmatrix} \begin{bmatrix} A_{s2, j} \\ B_{s2, j} \\ A_{s3, j} \\ B_{s3, j} \end{bmatrix} = \begin{bmatrix} -E_{10}(n_2, b) \cdot (A_{i1, n2}^* + A_{r4, n2}^*) \\ -E_{10}(n_2, b) \cdot B_{r4, n2}^* \\ -E_{12}(n_2, b) \cdot (A_{i1, n2}^* + A_{r4, n2}^*) \\ -E_{12}(n_2, b) \cdot B_{r4, n2}^* \end{bmatrix} \quad (32)$$

对于上述无穷阶线性方程组需要进行截断求解，之后可得到待定系数 $A_{s2, n2}$ 、 $B_{s2, n2}$ 、 $A_{s3, n2}$ 、 $B_{s3, n2}$ 的具体数值，进而求解可得介质中的位移场，具体求解过程限于篇幅，本文不再赘述。

4 分析与讨论

4.1 解答收敛性分析

为了综合分析各个因素的影响，文章引入无量纲频率 $\eta = \omega a / \pi \beta = ka / \pi = 2a / \lambda$ 。为了验证问题解的有效性，选取水平平行双圆衬砌隧洞的几何和物理力学参数分别为 $b/a=1.1$ 、 $d_{12}/a=20$ 、 $d_{23}/a=3.5$ 、 $D/a=2$ 、 $\beta_1/\beta=5/2$ 、 $\rho_1/\rho=2.5/1.6$ ，以及无量纲频率 $\eta=2$ 的情况下，左隧洞和右隧洞内外边界径向应力集中因子在不同截断项数情况下的收敛精度进行计算，如图3和图4所示，其中径向应力集中因

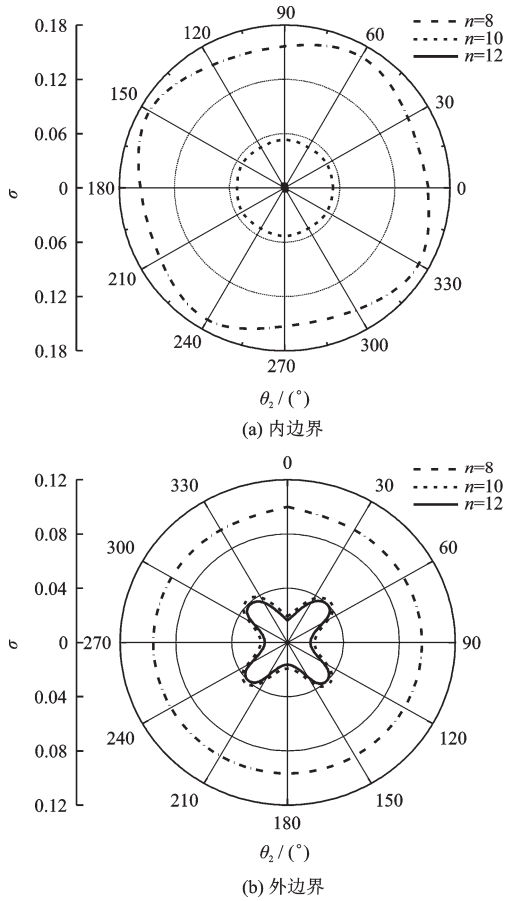


图3 左隧洞衬砌边界径向应力集中因子($\eta=2$)

Fig.3 Radial stress concentration factor of the left tunnel lined boundary ($\eta=2$)

子被定义为:

$$\sigma = \left| \frac{\sigma_r}{\sigma_0} \right| \quad (33)$$

其中, $\sigma_r = \mu_1 \frac{\partial W_{LL}}{\partial r_2}$, 是左隧洞介质内任意点的应力; $\sigma_0 = \mu \frac{\partial W_{r1}}{\partial r_1} = \mu k H_1^{(1)}(kr_1)$, 是入射波在无隧洞介质内任意点处产生的应力。

图5为径向应力集中因子计算示意图。当 $r_2 = b, r_1 = r'_1$ 时, 式(33)表示左隧洞外边界径向应力集中因子; 当 $r_2 = a, r_1 = r'_{1f}$ 时, 式(33)表示左隧洞内边界径向应力集中因子, 其它隧洞内外边界处径向应力集中因子表示方法类似。

从上图中可以看出, 内边界应力 σ 值随着截断项数 n 取值的增大而减小, 且减小趋势迅速并最终趋向于零, 衬砌内边界的零应力边界条件能够得到很好的满足; 外边界应力 σ 值随着截断项数 n 取值的增大而减小, 且减小趋势迅速并最终趋于稳定值, 衬砌外边界的应力稳定条件得到了较好的满

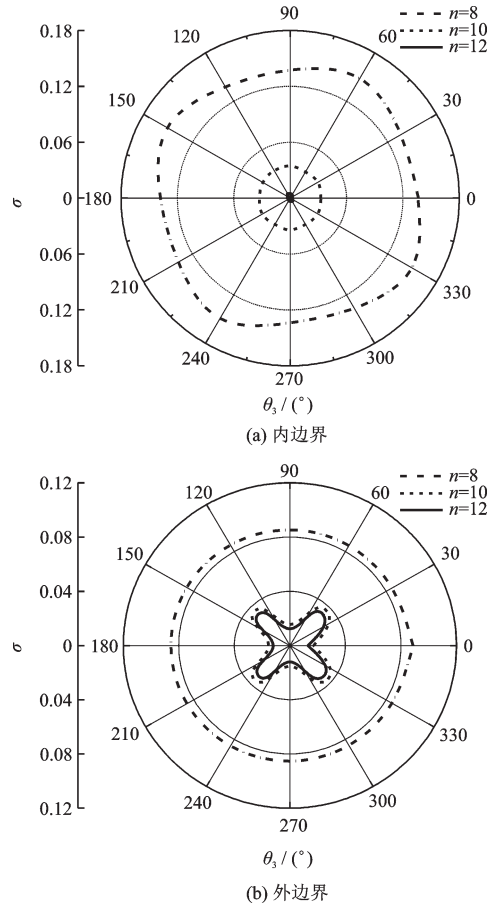


图4 右隧洞衬砌边界径向应力集中因子($\eta=2$)

Fig.4 Radial stress concentration factor of the right tunnel lined boundary($\eta=2$)

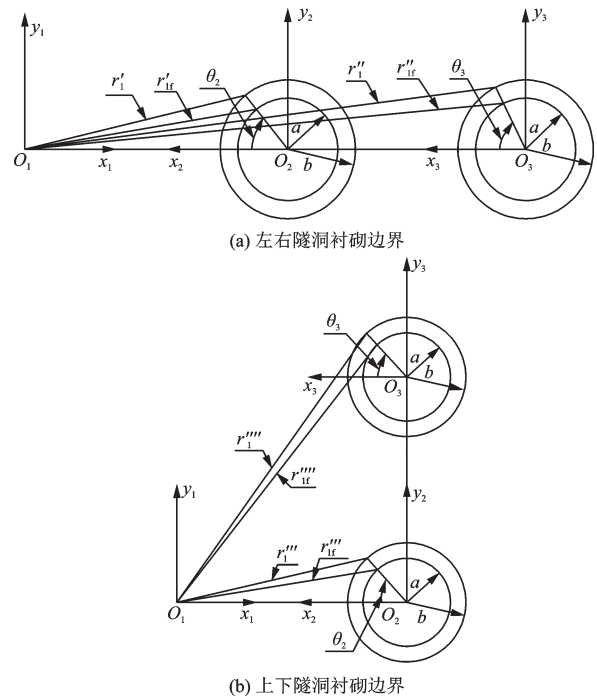


图5 径向应力集中因子计算示意

Fig.5 Schematic diagram of calculation of radial stress concentration factor

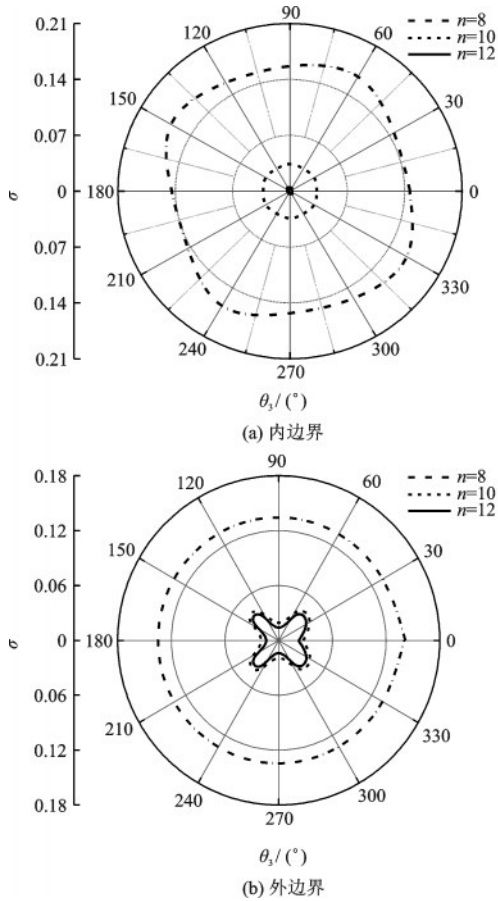


图6 上隧洞衬砌边界径向应力集中因子($\eta=2$)

Fig.6 Radial stress concentration factor of the upper tunnel lined boundary($\eta=2$)

足。因此,当截断项数取值很大时,边界条件就会得到较好地满足,解答的精度趋向于正确解,解的收敛性得到验证。

4.2 参数分析

由于篇幅所限,这里仅以模型1(水平方向平行布置双圆衬砌隧洞)为例,在相关参数(几何参数,力学参数)取值不同的情况下,对附近场地动力响应的影响进行分析。

为了分析衬砌刚度的影响,当无量纲频率 $\eta=1$ 时,取几何参数: $b/a=1.1$ 、 $d_{12}/a=20$ 、 $d_{23}/a=3.5$ 、 $D/a=2$,取力学参数:同性衬砌($\beta_1/\beta=1$ 、 $\rho_1/\rho=1$)、刚性衬砌($\beta_1/\beta=5/2$ 、 $\rho_1/\rho=2.5/1.6$)、柔性衬砌($\beta_1/\beta=2/5$ 、 $\rho_1/\rho=1.6/2.5$)的情形下,位移 W_L/W 值在不同深度 z/a 处沿水平方向的变化曲线,如图8所示。由于采用无量纲化处理,位移值取 W_L/W 的比值,水平方向和深度方向位置坐标分别取为 x/a 和 z/a 的比值。从图中可以看出,隧洞的衬砌结构

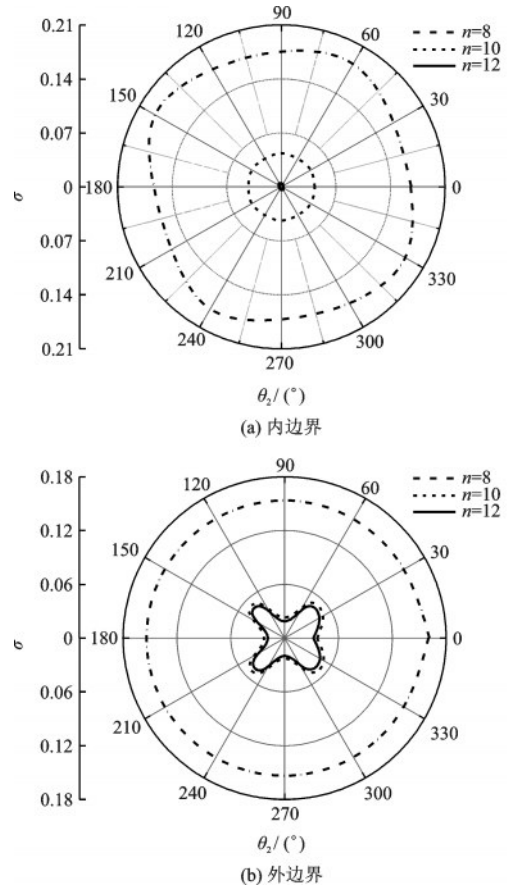


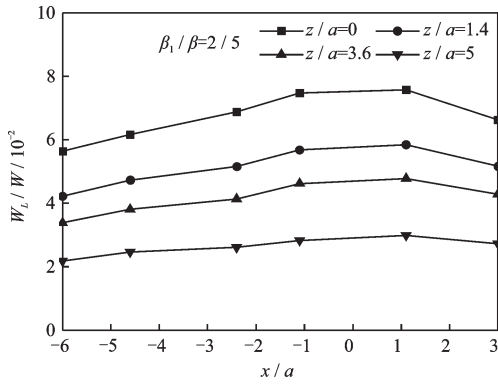
图7 下隧洞衬砌边界径向应力集中因子($\eta=2$)

Fig.7 Radial stress concentration factor of the lower tunnel lined boundary($\eta=2$)

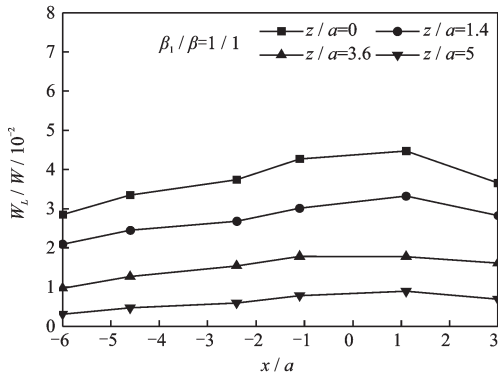
会对附近场地的动力响应带来显著的影响,并且附近场地的动力响应与衬砌自身的刚度有着密切的关系。当衬砌刚度由柔性变为刚性时,附近土体的位移幅值呈减小趋势。当参数取为刚性衬砌($\beta_1/\beta=5/2$ 、 $\rho_1/\rho=2.5/1.6$)时,隧洞附近土体的位移幅值沿深度方向减小趋势较为迅速,且最大幅度约为59.5%,而在水平方向上,靠近隧洞附近场地运动受到的影响更加显著。

取几何参数: $b/a=1.1$ 、 $d_{12}/a=20$ 、 $d_{23}/a=3.5$ 、 $D/a=2$;物理参数: $\beta_1/\beta=5/2$ 、 $\rho_1/\rho=2.5/1.6$ 时,在无量纲频率 $\eta=0.1$ 、0.5、1和2的情况下,隧洞附近场地土体位移幅值的变化曲线如图9所示。可以看出,当入射频率由低频变为高频时,附近土体的位移幅值呈增大趋势。在水平方向,当 $\eta=0.1$ 时,附近土体的位移幅值变化趋势比较小;当 $\eta=2$ 时,相对于右侧隧洞,左侧隧洞附近土体的位移幅值有明显增大,最大幅度约达到65%。

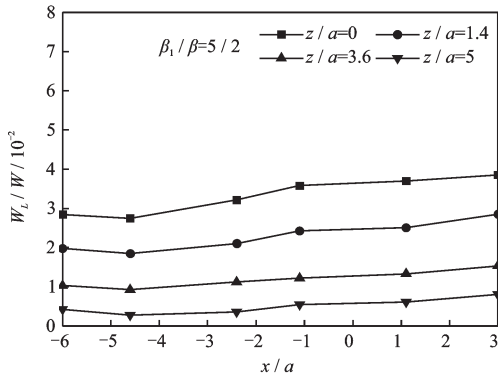
图10给出了在无量纲频率 $\eta=1$ 、 $b/a=1.1$ 、 $d_{12}/a=20$ 、 $\beta_1/\beta=5/2$ 、 $d_{23}/a=3$ 、 $\rho_1/\rho=2.5/1.6$ 时,隧



(a) 柔性衬砌



(b) 同性衬砌



(c) 刚性衬砌

图8 洞室埋深对附近场地位移幅值的影响在不同衬砌刚度下沿水平方向的变化曲线($\eta=1$)

Fig.8 Influence of tunnel depth on the displacement amplitude of nearby sites under different lining stiffness along the horizontal direction ($\eta=1$)

洞埋深分别为 $D/a=2.5$ 、 3.5 和 5 的情形下,水平平行双圆衬砌隧洞附近场地土体的位移幅值沿深度的变化曲线。可以看出,随着隧洞埋深增大,附近土体的位移幅值明显减小。当 $D/a=2.5$ 时,水平平行隧洞附近土体的位移幅值差在深度方向由 20% 减小为 17% ; 当 $D/a=5$ 时,水平平行隧洞附近土体的位移幅值差沿深度方向基本相等。

图 11 给出了在无量纲频率取值 $\eta=1$, $b/a=1.1$, $d_{12}/a=20$, $D/a=2.5$, $\beta_1/\beta=5/2$, $\rho_1/\rho=2.5/1.6$

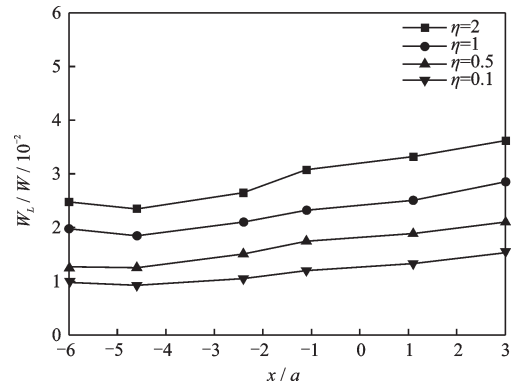


图9 入射频率对隧洞附近场地土体位移幅值的影响沿水平方向的变化曲线

Fig.9 Influence of incident frequency on the displacement amplitude of soil near the tunnel along the horizontal direction

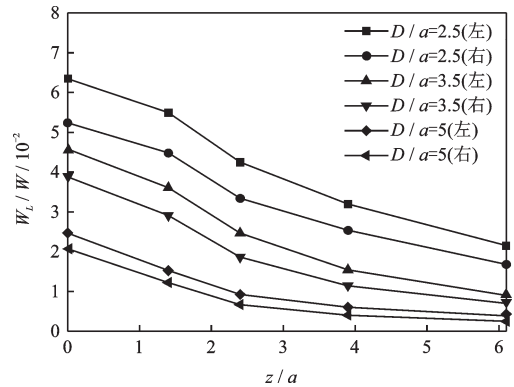


图10 埋深对隧洞附近场地土体位移幅值的影响沿深度方向的变化曲线($\eta=1$)

Fig.10 Influence of tunnel depth on the displacement amplitude of soil around the tunnel along the vertical direction ($\eta=1$)

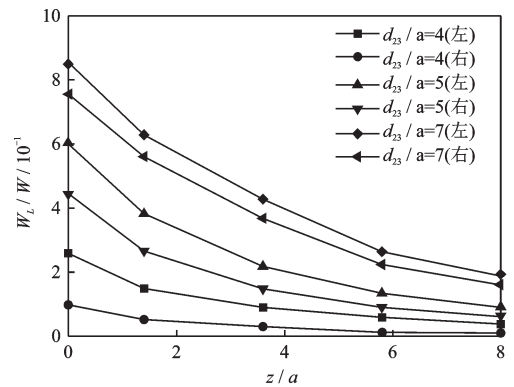


图11 隧洞间距对隧洞周围土体位移幅值沿深度的变化曲线($\eta=1$)

Fig.11 Variation curves of the displacement amplitude of the site along the depth of the tunnel with different burial spacings ($\eta=1$)

时,隧洞中心间距分别为 $d_{23}/a=4, 5$ 和 7 的情形下,水平平行双圆衬砌隧洞附近场地土体的位移幅值沿深度的变化曲线。从图中可以看出,双圆形衬砌隧洞附近场地土体的位移幅值随隧洞中心间距的增大而增大,特别是当中心间距从 8 m 增大到 14 m 时,附近场地土体的位移幅值有更明显的增大。当 $d_{23}/a=4$ 时,水平平行隧洞附近土体的位移幅值差在深度方向由 40% 减小为 20% ; 当 $d_{23}/a=7$ 时,水平平行隧洞附近土体的位移幅值差沿深度方向基本相等。

5 结 论

分析了弹性半空间中双圆衬砌隧洞对柱面 SH 波的散射问题,给出了弹性介质中位移场解析解,并对解的收敛性进行了验证。通过双圆衬砌隧洞的衬砌刚度、埋深、中心间距和入射频率等相关参数的分析,对隧洞附近场地的土体位移幅值在柱面 SH 波入射下沿水平方向和深度方向的变化规律进行了研究。其结果表明:

(1) 地下衬砌结构对附近场地的动力响应有显著的影响。与自由场相比较, $\beta_1/\beta=2/5$ 时在沿深度方向上柔性衬砌隧洞附近场地土体的位移幅值减小很迅速,最大减小幅度约为 59.5% , 在沿水平方向上,靠近隧洞附近场地土体的位移幅值受影响越显著; 而 $\beta_1/\beta=5/2$ 时刚性衬砌附近土体的位移幅值在深度方向的最大减小幅度约为 90% , 在水平方向变化趋势较小。

(2) 入射 SH 波的频率对衬砌附近场地的动力响应也有着重要影响。在水平方向,低频时双隧洞附近土体的位移幅值变化趋势较小; 而高频时,相对于右侧隧洞,左侧隧洞附近土体的位移幅值有明显增大,最大幅度约达到 65% 。

(3) 双衬砌隧洞的埋深和中心间距对附近场地动力响应的影响表现为:埋深较浅 ($D/a=2.5$) 时,双隧洞附近土体的位移幅值差在深度方向由 20% 减小为 17% ; 埋深较深 ($D/a=5$) 时,双隧洞附近土体的位移幅值差沿深度方向基本相等; 中心间距较小 ($d_{23}/a=4$) 时,双隧洞附近土体的位移幅值差在深度方向由 40% 减小为 20% , 中心间距较大 ($d_{23}/a=7$) 时,双隧洞附近土体的位移幅值差沿深度方向基本相等。

附录 A

$$A_{i1,n2}^* = \epsilon_{n_2} \cdot H_{n_2}^{(1)}(kd_{12}) \quad (\text{A.1})$$

$$A_{s3,n2}^* = \sum_{n_3=0}^{+\infty} A_{s3,n3} \cdot E_{5H}^{-32} \quad (\text{A.2})$$

$$B_{s3,n2}^* = \sum_{n_3=0}^{+\infty} B_{s3,n3} \cdot E_{5H}^{+32} \quad (\text{A.3})$$

$$A_{r4,n2}^* = \epsilon_{n_2} \cdot H_{n_2}^{(1)}(kd_{24}) \cdot \cos(n_2\varphi_4) \quad (\text{A.4})$$

$$B_{r4,n2}^* = \epsilon_{n_2} \cdot H_{n_2}^{(1)}(kd_{24}) \cdot \sin(n_2\varphi_4) \quad (\text{A.5})$$

$$A_{s5,n2}^* = \sum_{n_5=0}^{+\infty} (A_{s5,n5} \cdot E_{1H}^{+52} + B_{s5,n5} \cdot E_{2H}^{+52}) \quad (\text{A.6})$$

$$B_{s5,n2}^* = \sum_{n_5=0}^{+\infty} (B_{s5,n5} \cdot E_{1H}^{-52} - A_{s5,n5} \cdot E_{2H}^{-52}) \quad (\text{A.7})$$

$$A_{s6,n2}^* = \sum_{n_6=0}^{+\infty} (A_{s6,n6} \cdot E_{3H}^{-62} + B_{s6,n6} \cdot E_{4H}^{-62}) \quad (\text{A.8})$$

$$B_{s6,n2}^* = \sum_{n_6=0}^{+\infty} (A_{s6,n6} \cdot E_{4H}^{+62} + B_{s6,n6} \cdot E_{3H}^{+62}) \quad (\text{A.9})$$

$$E_{1H}^{\pm ij} = \frac{\epsilon_{n_2}}{2} \cdot \left[H_{n_j+n_i}(d_{25}) \cdot \cos\left(\frac{n_j-n_i}{2}\pi\right) \pm (-1)^{n_i} \cdot H_{n_j-n_i}(d_{25}) \cdot \cos\left(\frac{n_j+n_i}{2}\pi\right) \right] \quad (\text{A.10})$$

$$E_{2H}^{\pm ij} = \frac{\epsilon_{n_2}}{2} \cdot \left[-H_{n_j+n_i}(d_{25}) \cdot \sin\left(\frac{n_j-n_i}{2}\pi\right) \pm (-1)^{n_i} \cdot H_{n_j-n_i}(d_{25}) \cdot \sin\left(\frac{n_j+n_i}{2}\pi\right) \right] \quad (\text{A.11})$$

$$E_{3H}^{\pm ij} = \frac{\epsilon_{n_2}}{2} \cdot [-H_{n_j+n_i}(d_{26}) \cdot \cos(n_j+n_i)\varphi_6 \pm (-1)^{n_i} \cdot H_{n_j-n_i}(d_{26}) \cdot \cos(n_j-n_i)\varphi_6] \quad (\text{A.12})$$

$$E_{4H}^{\pm ij} = \frac{\epsilon_{n_2}}{2} \cdot [\pm H_{n_j+n_i}(d_{26}) \cdot \sin(n_j+n_i)\varphi_6 + (-1)^{n_i} \cdot H_{n_j-n_i}(d_{26}) \cdot \sin(n_j-n_i)\varphi_6] \quad (\text{A.13})$$

$$E_{5H}^{\pm ij} = \frac{\epsilon_{n_2}}{2} \cdot [\pm H_{n_j+n_i}(d_{23}) - (-1)^{n_i} \cdot H_{n_j-n_i}(d_{23})] \quad (\text{A.14})$$

$$E_{6J}^{\pm ij} = \frac{\epsilon_{n_2}}{2} \cdot [\pm J_{n_j+n_i}(d_{23}) - (-1)^{n_i} \cdot J_{n_j-n_i}(d_{23})] \quad (\text{A.15})$$

$$G_1(k_1r_2) = H_{n_2}^{(1)}(k_1r_2) - \frac{E_1(n_2,a)}{E_2(n_2,a)} \cdot J_{n_2}(k_1r_2) \quad (\text{A.16})$$

$$C_{L3,n2}^* = \sum_{n_3=0}^{+\infty} C_{L3,n3} (E_{5H}^{-32} - \frac{E_3(n_3,a)}{E_4(n_3,a)} E_{6J}^{-32}) \quad (\text{A.17})$$

$$D_{L3,n2}^* = \sum_{n_3=0}^{+\infty} D_{L3,n3} (E_{5H}^{+32} - \frac{E_3(n_3,a)}{E_4(n_3,a)} E_{6J}^{+32}) \quad (\text{A.18})$$

$$E_1(n_2,a) = n_2 H_{n_2}^{(1)}(k_1a) - k_1a \cdot H_{n_2+1}^{(1)}(k_1a) \quad (\text{A.19})$$

$$E_2(n_2,a) = n_2 J_{n_2}(k_1a) - k_1a \cdot J_{n_2+1}(k_1a) \quad (\text{A.20})$$

$$E_3(n_3, a) = n_3 H_{n_3}^{(1)}(k_1 a) - k_1 a \cdot H_{n_3+1}^{(1)}(k_1 a) \quad (\text{A.21})$$

$$E_4(n_3, a) = n_3 J_{n_3}(k_1 a) - k_1 a \cdot J_{n_3+1}(k_1 a) \quad (\text{A.22})$$

$$E_5(n_2, b) = n_2 H_{n_2}^{(1)}(kb) - kb \cdot H_{n_2+1}^{(1)}(kb) \quad (\text{A.23})$$

$$E_6(n_2, b) = n_2 J_{n_2}(kb) - kb \cdot J_{n_2+1}(kb) \quad (\text{A.24})$$

$$E_7(n_2, b) = n_2 H_{n_2}^{(1)}(k_1 b) - k_1 b \cdot H_{n_2+1}^{(1)}(k_1 b) \quad (\text{A.25})$$

$$E_8(n_2, b) = n_2 J_{n_2}(k_1 b) - k_1 b \cdot J_{n_2+1}(k_1 b) \quad (\text{A.26})$$

$$E_9(n_2, b) = E_7(n_2, b) - \frac{E_1(n_2, a)}{E_2(n_2, a)} \cdot E_8(n_2, b) \quad (\text{A.27})$$

$$E_{10}(n_2, b) = E_6(n_2, b) - \frac{\mu_1}{\mu} \cdot E_9(n_2, b) \cdot \frac{J_{n_2}(kb)}{G_1(k_1 b)} \quad (\text{A.28})$$

$$E_{11}(n_2, b) = E_5(n_2, b) - \frac{\mu_1}{\mu} \cdot E_9(n_2, b) \cdot \frac{H_{n_2}^{(1)}(kb)}{G_1(k_1 b)} \quad (\text{A.29})$$

$$E_{12}(n_2, b) = E_6(n_2, b) - \frac{\mu_1}{\mu} \cdot E_8(n_2, b) \cdot \frac{J_{n_2}(kb)}{J_{n_2}(k_1 b)} \quad (\text{A.30})$$

$$E_{13}(n_2, b) = E_5(n_2, b) - \frac{\mu_1}{\mu} \cdot E_8(n_2, b) \cdot \frac{H_{n_2}^{(1)}(kb)}{J_{n_2}(k_1 b)} \quad (\text{A.31})$$

$$E_{11} = E_{10}(n_2, b) \cdot E_{1H}^{+j^2} + E_{11}(n_2, b) \quad (\text{A.32})$$

$$E_{12} = E_{10}(n_2, b) \cdot E_{2H}^{+j^2} \quad (\text{A.33})$$

$$E_{13} = E_{10}(n_2, b) \cdot (E_{5H}^{-j^2} + E_{3H}^{-j^2}) \quad (\text{A.34})$$

$$E_{14} = E_{10}(n_2, b) \cdot E_{4H}^{-j^2} \quad (\text{A.35})$$

$$E_{21} = E_{10}(n_2, b) \cdot (-E_{2H}^{-j^2}) \quad (\text{A.36})$$

$$E_{22} = E_{10}(n_2, b) \cdot E_{1H}^{-j^2} + E_{11}(n_2, b) \quad (\text{A.37})$$

$$E_{23} = E_{10}(n_2, b) \cdot E_{4H}^{+j^2} \quad (\text{A.38})$$

$$E_{24} = E_{10}(n_2, b) \cdot (E_{5H}^{+j^2} + E_{3H}^{+j^2}) \quad (\text{A.39})$$

$$E_{31} = E_{12}(n_2, b) \cdot E_{1H}^{+j^2} + E_{13}(n_2, b) \quad (\text{A.40})$$

$$E_{32} = E_{12}(n_2, b) \cdot E_{2H}^{+j^2} \quad (\text{A.41})$$

$$E_{33} = E_{12}(n_2, b) \cdot (E_{5H}^{-j^2} + E_{3H}^{-j^2}) \quad (\text{A.42})$$

$$E_{34} = E_{12}(n_2, b) \cdot E_{4H}^{-j^2} \quad (\text{A.43})$$

$$E_{41} = E_{12}(n_2, b) \cdot (-E_{2H}^{-j^2}) \quad (\text{A.44})$$

$$E_{42} = E_{12}(n_2, b) \cdot E_{1H}^{-j^2} + E_{13}(n_2, b) \quad (\text{A.45})$$

$$E_{43} = E_{12}(n_2, b) \cdot E_{4H}^{+j^2} \quad (\text{A.46})$$

$$E_{44} = E_{12}(n_2, b) \cdot (E_{5H}^{+j^2} + E_{3H}^{+j^2}) \quad (\text{A.47})$$

附录 B

$$A_{i1, n_2}^* = \epsilon_{n_2} \cdot H_{n_2}^{(1)}(kd_{12}) \quad (\text{B.1})$$

$$A_{s3, n_2}^* = \sum_{n_3=0}^{+\infty} (A_{s3, n_3} \cdot E_{1H}^{+32} + B_{s3, n_3} \cdot E_{2H}^{+32}) \quad (\text{B.2})$$

$$B_{s3, n_2}^* = \sum_{n_3=0}^{+\infty} (B_{s3, n_3} \cdot E_{1H}^{-32} - A_{s3, n_3} \cdot E_{2H}^{-32}) \quad (\text{B.3})$$

$$A_{r4, n_2}^* = \epsilon_{n_2} \cdot H_{n_2}^{(1)}(kd_{24}) \cdot \cos(n_2 \varphi_4) \quad (\text{B.4})$$

$$B_{r4, n_2}^* = \epsilon_{n_2} \cdot H_{n_2}^{(1)}(kd_{24}) \cdot \sin(n_2 \varphi_4) \quad (\text{B.5})$$

$$A_{s5, n_2}^* = \sum_{n_5=0}^{+\infty} (A_{s5, n_5} \cdot E_{3H}^{+52} + B_{s5, n_5} \cdot E_{4H}^{+52}) \quad (\text{B.6})$$

$$B_{s5, n_2}^* = \sum_{n_4=0}^{+\infty} (B_{s5, n_5} \cdot E_{3H}^{-52} - A_{s5, n_5} \cdot E_{4H}^{-52}) \quad (\text{B.7})$$

$$A_{s6, n_2}^* = \sum_{n_6=0}^{+\infty} (A_{s6, n_6} \cdot E_{5H}^{+62} + B_{s6, n_6} \cdot E_{6H}^{+62}) \quad (\text{B.8})$$

$$B_{s6, n_2}^* = \sum_{n_6=0}^{+\infty} (B_{s6, n_6} \cdot E_{5H}^{-62} - A_{s6, n_6} \cdot E_{6H}^{-62}) \quad (\text{B.9})$$

$$E_{1H}^{\pm ij} = \frac{\epsilon_{n_2}}{2} \cdot \left[H_{n_j+n_i}(d_{23}) \cdot \cos\left(\frac{n_j-n_i}{2}\pi\right) \pm (-1)^{n_i} \cdot H_{n_j-n_i}(d_{23}) \cdot \cos\left(\frac{n_j+n_i}{2}\pi\right) \right] \quad (\text{B.10})$$

$$E_{2H}^{\pm ij} = \frac{\epsilon_{n_2}}{2} \cdot \left[-H_{n_j+n_i}(d_{23}) \cdot \sin\left(\frac{n_j-n_i}{2}\pi\right) \pm (-1)^{n_i} \cdot H_{n_j-n_i}(d_{23}) \cdot \sin\left(\frac{n_j+n_i}{2}\pi\right) \right] \quad (\text{B.11})$$

$$E_{3H}^{\pm ij} = \frac{\epsilon_{n_2}}{2} \cdot \left[H_{n_j+n_i}(d_{25}) \cdot \cos\left(\frac{n_j-n_i}{2}\pi\right) \pm (-1)^{n_i} \cdot H_{n_j-n_i}(d_{25}) \cdot \cos\left(\frac{n_j+n_i}{2}\pi\right) \right] \quad (\text{B.12})$$

$$E_{4H}^{\pm ij} = \frac{\epsilon_{n_2}}{2} \cdot \left[-H_{n_j+n_i}(d_{25}) \cdot \sin\left(\frac{n_j-n_i}{2}\pi\right) \pm (-1)^{n_i} \cdot H_{n_j-n_i}(d_{25}) \cdot \sin\left(\frac{n_j+n_i}{2}\pi\right) \right] \quad (\text{B.13})$$

$$E_{5H}^{\pm ij} = \frac{\epsilon_{n_2}}{2} \cdot \left[H_{n_j+n_i}(d_{26}) \cdot \cos\left(\frac{n_j-n_i}{2}\pi\right) \pm (-1)^{n_i} \cdot H_{n_j-n_i}(d_{26}) \cdot \cos\left(\frac{n_j+n_i}{2}\pi\right) \right] \quad (\text{B.14})$$

$$E_{6H}^{\pm ij} = \frac{\epsilon_{n_2}}{2} \cdot \left[-H_{n_j+n_i}(d_{26}) \cdot \sin\left(\frac{n_j-n_i}{2}\pi\right) \pm (-1)^{n_i} \cdot H_{n_j-n_i}(d_{26}) \cdot \sin\left(\frac{n_j+n_i}{2}\pi\right) \right] \quad (\text{B.15})$$

$$E_{7J}^{\pm ij} = \frac{\epsilon_{n_2}}{2} \cdot \left[J_{n_j+n_i}(d_{23}) \cdot \cos\left(\frac{n_j-n_i}{2}\pi\right) \pm (-1)^{n_i} \cdot J_{n_j-n_i}(d_{23}) \cdot \cos\left(\frac{n_j+n_i}{2}\pi\right) \right] \quad (\text{B.16})$$

$$E_{8J}^{\pm ij} = \frac{\epsilon_{n_2}}{2} \cdot \left[-J_{n_j+n_i}(d_{23}) \cdot \sin\left(\frac{n_j-n_i}{2}\pi\right) \pm (-1)^{n_i} \cdot J_{n_j-n_i}(d_{23}) \cdot \sin\left(\frac{n_j+n_i}{2}\pi\right) \right] \quad (\text{B.17})$$

$$G_1(k_1 r_2) = H_{n_2}^{(1)}(k_1 r_2) - \frac{E_1(n_2, a)}{E_2(n_2, a)} \cdot J_{n_2}(k_1 r_2) \quad (\text{B.18})$$

$$C_{L3,n2}^* = \sum_{n_3=0}^{+\infty} \left[C_{L3,n3} \cdot \left(E_{1H}^{+32} + \frac{E_3(n_3,a)}{E_4(n_3,a)} E_{7J}^{+32} \right) + D_{L3,n3} \cdot \left(E_{2H}^{+32} + \frac{E_3(n_3,a)}{E_4(n_3,a)} E_{8J}^{+32} \right) \right] \quad (B.19)$$

$$D_{L3,n2}^* = \sum_{n_3=0}^{+\infty} \left[C_{L3,n3} \cdot \left(\frac{E_3(n_3,a)}{E_4(n_3,a)} E_{8J}^{-32} - E_{2H}^{-32} \right) + D_{L3,n3} \cdot \left(E_{1H}^{-32} - \frac{E_3(n_3,a)}{E_4(n_3,a)} E_{7J}^{-32} \right) \right] \quad (B.20)$$

$$E_1(n_2, a) = n_2 H_{n_2}^{(1)}(k_1 a) - k_1 a \cdot H_{n_2+1}^{(1)}(k_1 a) \quad (B.21)$$

$$E_2(n_2, a) = n_2 J_{n_2}(k_1 a) - k_1 a \cdot J_{n_2+1}(k_1 a) \quad (B.22)$$

$$E_3(n_3, a) = n_3 H_{n_3}^{(1)}(k_1 a) - k_1 a \cdot H_{n_3+1}^{(1)}(k_1 a) \quad (B.23)$$

$$E_4(n_3, a) = n_3 J_{n_3}(k_1 a) - k_1 a \cdot J_{n_3+1}(k_1 a) \quad (B.24)$$

$$E_5(n_2, b) = n_2 H_{n_2}^{(1)}(k b) - k b \cdot H_{n_2+1}^{(1)}(k b) \quad (B.25)$$

$$E_6(n_2, b) = n_2 J_{n_2}(k b) - k b \cdot J_{n_2+1}(k b) \quad (B.26)$$

$$E_7(n_2, b) = n_2 H_{n_2}^{(1)}(k_1 b) - k_1 b \cdot H_{n_2+1}^{(1)}(k_1 b) \quad (B.27)$$

$$E_8(n_2, b) = n_2 J_{n_2}(k_1 b) - k_1 b \cdot J_{n_2+1}(k_1 b) \quad (B.28)$$

$$E_9(n_2, b) = E_7(n_2, b) - \frac{E_1(n_2, a)}{E_2(n_2, a)} \cdot E_8(n_2, b) \quad (B.29)$$

$$E_{10}(n_2, b) = E_6(n_2, b) - \frac{\mu_1}{\mu} \cdot E_9(n_2, b) \cdot \frac{J_{n_2}(k b)}{G_1(k_1 b)} \quad (B.30)$$

$$E_{11}(n_2, b) = E_5(n_2, b) - \frac{\mu_1}{\mu} \cdot E_9(n_2, b) \cdot \frac{H_{n_2}^{(1)}(k b)}{G_1(k_1 b)} \quad (B.31)$$

$$E_{12}(n_2, b) = E_6(n_2, b) - \frac{\mu_1}{\mu} \cdot E_8(n_2, b) \cdot \frac{J_{n_2}(k b)}{J_{n_2}(k_1 b)} \quad (B.32)$$

$$E_{13}(n_2, b) = E_5(n_2, b) - \frac{\mu_1}{\mu} \cdot E_8(n_2, b) \cdot \frac{H_{n_2}^{(1)}(k b)}{J_{n_2}(k_1 b)} \quad (B.33)$$

$$E_{11} = E_{10}(n_2, b) \cdot E_{3H}^{+j2} + E_{11}(n_2, b) \quad (B.34)$$

$$E_{12} = E_{10}(n_2, b) \cdot E_{4H}^{+j2} \quad (B.35)$$

$$E_{13} = E_{10}(n_2, b) \cdot (E_{1H}^{+j2} + E_{5H}^{+j2}) \quad (B.36)$$

$$E_{14} = E_{10}(n_2, b) \cdot (E_{2H}^{+j2} + E_{6H}^{+j2}) \quad (B.37)$$

$$E_{21} = E_{10}(n_2, b) \cdot (-E_{5H}^{-j2}) \quad (B.38)$$

$$E_{22} = E_{10}(n_2, b) \cdot E_{3H}^{-j2} + E_{11}(n_2, b) \quad (B.39)$$

$$E_{23} = E_{10}(n_2, b) \cdot (-E_{2H}^{-j2} - E_{6H}^{-j2}) \quad (B.40)$$

$$E_{24} = E_{10}(n_2, b) \cdot (E_{1H}^{-j2} + E_{5H}^{-j2}) \quad (B.41)$$

$$E_{31} = E_{12}(n_2, b) \cdot E_{3H}^{+j2} + E_{13}(n_2, b) \quad (B.42)$$

$$E_{32} = E_{12}(n_2, b) \cdot E_{4H}^{+j2} \quad (B.43)$$

$$E_{33} = E_{12}(n_2, b) \cdot (E_{1H}^{+j2} + E_{5H}^{+j2}) \quad (B.44)$$

$$E_{34} = E_{12}(n_2, b) \cdot (E_{2H}^{+j2} + E_{6H}^{+j2}) \quad (B.45)$$

$$E_{41} = E_{12}(n_2, b) \cdot (-E_{5H}^{-j2}) \quad (B.46)$$

$$E_{42} = E_{12}(n_2, b) \cdot E_{3H}^{-j2} + E_{13}(n_2, b) \quad (B.47)$$

$$E_{43} = E_{12}(n_2, b) \cdot (-E_{2H}^{-j2} - E_{6H}^{-j2}) \quad (B.48)$$

$$E_{44} = E_{12}(n_2, b) \cdot (E_{1H}^{-j2} + E_{5H}^{-j2}) \quad (B.49)$$

参考文献:

- [1] Pao Y H, Mow C C. Diffraction of elastic waves and dynamic stress concentrations [M]. New York: Crane Russak and Company, 1973.
- [2] Lee V W, Karl J. Diffraction of SV waves by underground, circular, cylindrical cavities [J]. Soil Dynamics and Earthquake Engineering, 1992, 11: 445-456.
- [3] Moore I D, Guan F. Three-dimensional dynamic response of lined tunnels due to incident seismic waves [J]. Earthquake Engineering & Structural Dynamics, 1996, 25(4): 357-369.
- [4] Lee V W. A series solution for surface motion amplification due to underground twin tunnels: incident SV waves [J]. Earthquake Engineering and Engineering Vibration, 2003, 2(2): 289-298.
- [5] Liu Q J, Zhao M J, Wang L H. Scattering of plane P, SV or Rayleigh waves by a shallow lined tunnel in an elastic half space [J]. Soil Dynamics & Earthquake Engineering, 2013, 49(6): 52-63.
- [6] 梁建文, 丁美, 杜金金. 柱面 SH 波在地下圆形衬砌洞室周围散射解析解 [J]. 地震工程与工程震动, 2013, 33(1): 1-7.
Liang J W, Ding M, Du J J. Diffraction of cylindrical SH waves around circular lined cavity: analytical solution [J]. Earthquake Engineering and Engineering Vibration, 2013, 33(1): 1-7. (in Chinese)
- [7] Xu H, Li T B, Xu J S, et al. Dynamic response of underground circular lining tunnels subjected to incident P waves [J]. Mathematical Problems in Engineering, 2014 (4): 1-11.
- [8] Liu Zh X, Liu L. An IBEM solution to the scattering of plane SH-waves by a lined tunnel in elastic wedge space [J]. Earthquake Science, 2015, 28(1): 71-86.
- [9] 梁建文, 纪晓东, Lee V W. 地下圆形衬砌隧道对沿线地震动的影响 (I): 级数解 [J]. 岩土力学, 2005, 26(4): 520-524.
Liang J W, Ji X D, Lee V W. Effect of an underground lining tunnel on ground motion (I): series solution [J]. Rock and Soil Mechanics, 2005, 26(4): 520-524. (in Chinese)
- [10] 梁建文, 纪晓东, Lee V W. 地下圆形衬砌隧道对沿线

- 地震动的影响(II):数值结果[J]. 岩土力学, 2005, 26(5): 687-692.
- Liang J W, Ji X D, Lee V W. Effect of an underground lining tunnel on ground motion (II) : numerical results [J]. Rock and Soil Mechanics, 2005, 26(5): 687-692. (in Chinese)
- [11] Liang J W, Chen J Q, Ba Zh N. 3D scattering of obliquely incident SH waves by a cylindrical cavity in layered elastic half-space (I) : methodology and verification [J]. Acta Seismologica Sinica, 2012, 34 (6) : 785-792.
- [12] Liang J W, Chen J Q, Ba Zh N. 3D scattering of obliquely incident SH waves by a cylindrical cavity in layered elastic half-space (II) : numerical results and analysis [J]. Acta Seismologica Sinica, 2013, 35(2) : 173-183.
- [13] 梁建文,胡淞淋,刘中宪,等. 平面SH波在弹性半空间中三维洞室周围的散射[J]. 地震工程与工程震动, 2015, 35(4): 40-50.
- Liang J W, Hu S L, Liu Zh X, et al. Scattering of plane SH waves around three dimensional caverns in elastic half space [J]. Earthquake Engineering and Engineering Vibration, 2015, 35(4): 40-50. (in Chinese)
- [14] 梁建文,胡淞淋,刘中宪,等. 平面SV波入射下弹性半空间中三维球形洞室的动力响应[J]. 岩土工程学报, 2016, 38(9): 1559-1568.
- Liang J W, Hu S L, Liu Zh X, et al. Dynamic response of three-dimensional spherical cavities in elastic half space under plane SV wave incident [J]. Journal of Geotechnical Engineering, 2016, 38 (9) : 1559-1568. (in Chinese)
- [15] Liang J W, Zhang H, Lee V W. A series solution for surface motion amplification due to underground twin tunnels: incident SV waves [J]. Earthquake Engineering and Engineering Vibration, 2003, 2(2): 289-298.
- [16] Liang J W, Zhang H, Lee V W. A series solution for surface motion amplification due to underground group cavities: Incident P waves [J]. Acta Seismologica Sinica (English Edition), 2004, 17(2): 296-307.
- [17] 梁建文,李艳恒, Lee V W. 地下洞室群对地面运动影响问题的级数解答: SH波入射 [J]. 岩土力学, 2006 (10):1663-1667,1672.
- Liang J W, Li Y H, Lee V W. A series solution for surface motion amplification due to underground twin tunnels: incident SH waves [J]. Rock and Soil Mechanics, 2006(10):1663-1667,1672. (in Chinese)
- [18] Alielahi H, Adampira M. Effect of twin-parallel tunnels on seismic ground response due to vertically in-plane waves [J]. International Journal of Rock Mechanics & Mining Sciences, 2016, 85: 67-83.
- [19] Liu Zh X, Wang Y R, Liang J W. Dynamic interaction of twin vertically overlapping lined tunnels in an elastic half space subjected to incident plane waves [J]. Earthquake Science, 2016, 29(3): 185-201.
- [20] 庞宾宾. 柱面SH波作用下圆形衬砌隧洞对附近场地动力响应的影响分析[D]. 兰州:兰州理工大学, 2018.
- Pang B B. Analysis of the influence of circular lining tunnel on dynamic response of nearby site under cylinder SH wave [D]. Lanzhou: Lanzhou University of Technology, 2018. (in Chinese)

(本文责编:赵霞)



(上接第 275 页)

- [20] Holland G J. An analytic model of the wind and pressure profiles in hurricanes [J]. Monthly Weather Review, 1980, 108(8): 1212-1218.
- [21] Smith R K (1968) The surface boundary layer of a hurricane. Tellus 20:473 - 483
- [22] Khare S P, Bonazzi A, West N, et al. On the modeling of over-ocean hurricane surface winds and their uncertainty [J]. Quarterly Journal of the Royal Meteorological Society: A Journal of the Atmospheric Sciences, Applied Meteorology and Physical Oceanography, 2009, 135(642): 1350-1365.
- [23] Vickery P J, Wadhwa D, Powell M D, et al. A hurricane boundary layer and wind field model for use in engineering applications [J]. Journal of Applied Meteorology and Climatology, 2009, 48(2): 381-405.
- [24] Powell M D, Vickery P J, Reinhold T A. Reduced drag coefficient for high wind speeds in tropical cyclones [J]. Nature, 2003, 422(6929): 279.
- [25] UCAR/NCAR-Earth Observing Laboratory. NCAR Airborne Vertical Atmospheric Profiling System (AVAPS). UCAR/NCAR - Earth Observing Laboratory, 1993, <https://doi.org/10.5065/D66W9848> Retrieved March 22, 2017.
- [26] Hock T F, Franklin J L. The NCAR GPS dropwindsonde [J]. Bulletin of the American Meteorological Society, 1999, 80(3), 407-420.